Mol. Cryst. Liq. Cryst., Vol. 527: pp. 72/[228]–79/[235], 2010

ISSN: 1542-1406 print/1563-5287 online
DOI: 10.1080/15421406.2010.486362

Taylor & Francis
Taylor & Francis Group

The Effect of the Size of $BaTiO_3$ Nanoparticles on the Electro-Optic Properties of Nematic Liquid Crystals

M. R. HERRINGTON, O. BUCHNEV, M. KACZMAREK, AND I. NANDHAKUMAR

School of Physics and Astronomy and School of Chemistry, University of Southampton, Southampton, UK

The size, size distribution and shape of ferroelectric $BaTiO_3$ nanoparticles were determined using three different imaging techniques. The nanoparticles fabricated by milling microcrystals were found to have sizes of 12 ± 3 nm, 15 ± 3 nm and 18 ± 3 nm. Liquid crystal suspensions with 1% concentration of nanoparticles were prepared and their dielectric and optical anisotropy were measured. It is shown that the largest particles lead to the strongest enhancement of dielectric and optical anisotropy, as compared with undoped liquid crystals.

Keywords Barium titanate; ferroelectric nanoparticles; nematic liquid crystal colloids

1. Introduction

Hybrid liquid crystal materials have attracted significant interest in recent years as they can increase the sensitivity to electric or magnetic fields, photorefractive or non-linear properties of the constituent materials. For example, silica nanoparticles in liquid crystals yield a strong reorientational effect [1] or gold nanoparticles show strong plasmonic resonance [2,3]. Hybrid systems typically include either solid state photorefractive windows [4], photoconductive polymer layers sandwiched with liquid crystals [5–7] or nanodopants suspended in liquid crystals. One type of such nanodopant are ferroelectric nanoparticles in nematic liquid crystals [8–11]. Ferroelectric nanoparticles, such as $Sn_2P_2S_6$ or $BaTiO_3$, show particularly strong modification of the host properties, such as increased phase transition temperatures, increased dielectric and optical anisotropy, which can be applied, for example, to the recording and storage of information and display technologies [12].

Although the effect of ferroelectric nanoparticles in liquid crystals has been studied by several different groups [8,10,11,13,14], to the best of our knowledge, there have been no reports on how the size or shape of such nanoparticles affects the electro-optic performance of liquid crystal suspensions. Of particular interest are particles in the

Address correspondence to I. Nandhakumar, School of Physics and Astronomy and School of Chemistry, University of Southampton, Southampton SO17 1BJ, UK. E-mail: m.r.herrington@phys.soton.ac.uk

region of 10–20 nm, which is regarded as the limit beyond which they are predicted to lose their ferroelectric properties [15]. Such small ferroelectric nanoparticles offer the advantage of modifying the electric response of the suspensions without reducing their high optical quality. One of the most successful methods to achieve 10–20 nm, but still ferroelectric, nanoparticles relies on milling of microcrystals. With other methods of synthesising ferroelectric $BaTiO_3$ particles, such as sol-gel, particles would have to be larger than 40 nm to remain ferroelectric [16]. To determine the effect of the $BaTiO_3$ nanoparticles on liquid crystal suspensions, their shape and size distribution have to be precisely measured. In order to achieve stable suspensions and to prevent nanoparticles aggregation, the nanoparticles have to be coated with surfactant. The presence of this surfactant, oleic acid, partially obscures the actual size of the particles. Therefore, different imaging techniques are used in this study to ensure the accurate determination of the nanoparticles' physical dimensions. The three different techniques selected for this investigation were: transmission electron microscopy (TEM), Super Sharp tip Atomic Force Microscopy (SSAFM) and Nanosight^{TM}, a dynamic light scattering technique. In this work we demonstrate the benefits of such comprehensive imaging approach to capture nanoparticles' physical parameters and show that the magnitude of enhanced dielectric and optical anisotropy is correlated with the size of particles.

2. Experimental Methods

Three samples of $BaTiO_3$ were prepared by two different milling techniques. First, micron sized $BaTiO_3$ particles were milled for 140 hours in a vibration mill mixed with a surfactant (oleic acid) and a solvent (heptane). The milled particles were then allowed to settle and precipitate. Finally, particles were taken from the top of the solution (sample A). The same procedure was followed using a planetary ball mill [17], however milling was carried out for either 12 hours (sample B) or 10 hours (sample C). For vibration milling, micron sized particles are placed in vessel with a large agate ball, the vessel is then vibrated and the micron size particles are ground down to nanoparticles over hundreds of hours. For planetary ball milling, the micron sized particles are placed in a vessel with several balls of zirconia. The vessel is rotated and high pulverization energy is achieved. Therefore, relatively short milling time is needed, typically 10 hours, to produce nanoparticles.

Three different techniques were used to characterise the particles produced: Transmission Electron Microscopy (TEM), Supersharp Atomic Force Microscopy (SSAFM) and Nanosight^{TM} a light scattering technique.

Substrates for TEM analysis were prepared by placing a drop of each sample onto carbon coated TEM grid and then dried in air. A Hitachi H7000 transmission electron microscope was used to obtain images with a resolution of 2 nm. AFM substrates were prepared by spinning a drop from one of the samples on a silicon wafer, cut to 1 cm $\times$ 1 cm, at 500 rpm for 3 seconds and then 2000 rpm for 10 seconds. The resulting wafers were placed in a Digital Instruments Multimode AFM with a supersharp AFM tip. This provided lateral resolution of 4 nm and a vertical resolution of 1 nm. Nanosight^{TM} measurements were taken using a Nanosight LM10. The solution of nanoparticles, dissolved in heptane, was added to the measurement chamber. The scattering method relies on illuminating the nanoparticles' solution with a laser beam and collecting the photons scattered by the nanoparticles out of the plane of the sample. A CCD camera is used to track the Brownian motion of the particles and accompanied software enabled us to determine their hydrodynamic diameter.

Suspensions of nanoparticles in liquid crystals were then prepared by doping liquid crystals TL205 and MLC6815 with samples A, B or C, respectively, so all the suspensions contained 1% (by weight) of nanoparticles. TL205 is a high birefringence liquid crystal ($n_e = 1.74$ and $n_o = 1.52$ measured at 589.3 nm), MLC6815 is a low birefringence liquid crystal with a refractive index closely matching that of silica ($n_e = 1.52$ and $n_o = 1.47$ measured at 589.3 nm). The suspensions were heated above the nematic-isotropic phase transition temperature and stirred for 24 hours to evaporate the solvent. The suspensions were then use to fill cells whose structure consisted of two ITO covered glass substrates. One substrate had a polyvinylcarbazole doped with fullerenes (PVK:C60) aligning layer and the other had polyimide (PI) layer. These alignment layers were gently rubbed to give a planar alignment.

The dielectric anisotropy and the refractive index anisotropy of the suspensions were then measured. The complex dielectric permittivity was measured using a Wayne Kerr Automatic precision bridge B905 at 1 kHz with an applied bias voltage increasing from 0 V to 50 V. Refractive index anisotropy measurements were taken using an electrically induced optical anisotropy method [18]. The cell was placed between crossed polarisers, with the cells director at 0 V aligned at 45° to each of the polarisers. The illuminating beam came from a 543.5 nm cw, HeNe laser with intensity of $2\,mW/cm^2$ The phase retardation between extraordinary and ordinary waves changed as the liquid crystal director reoriented with an applied electric field. The transmitted light intensity was monitored as the applied voltage was increased and the material birefringence was extracted from this measurement.

3. Results and Discussion

3.1. *Imaging of Nanoparticles*

The organic surfactant, oleic acid, which is necessary to produce stable suspensions of nanoparticles in liquid crystals leads to the impairment of contrast between the nanoparticles and the surrounding solvent. The surfactant is essential to prevent the agglomeration of nanoparticles into larger particles. Particle aggregates can disrupt the liquid crystal director, create defects and therefore decrease the optical quality of a cell. To overcome the problems with poor contrast, the original solution with nanoparticles had to be diluted further, in a larger volume of solvent. While this procedure could not completely remove oleic acid, in particular that directly bonded to the particles' surface, it helped in eliminating excess oleic acid. It also proved successful in obtaining AFM and TEM images of sufficient quality to determine the physical size of the particles.

Figure 1a presents a typical TEM image taken for sample B. The nanoparticles tend to have sharp and angular shape and edges. The same is observed for particles from sample C which are produced by the same milling technique. Particles from sample A (Fig. 1b) tend to have a much smoother appearance. In this way, the difference in surface roughness of nanoparticles produced via different milling was confirmed. This result is indeed consistent with the features of the two methods – vibration milling applying more moderate forces, but for longer time, than the planetary ball milling.

Particles measured for sample A were 15 ± 3 nm on average, but extra dilution in solvent prevented a robust histogram of the size distribution being generated. Sample B shows that there is a clear peak in size at 12 ± 3 nm. Sample C shows a

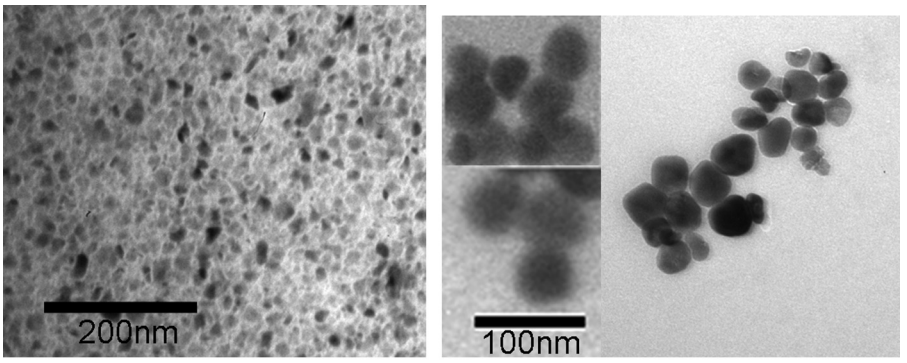

Figure 1. TEM images of ferroelectric Barium Titanate nanoparticles. (1a) Sample B particles, produced after 12 hours of grinding in a planetary ball mill. (1b) Sample A particles, produced after 140 hours of grinding a vibration mill.

clear peak at 12 ± 3 nm, as with sample B, however there is also a second peak observed at 18 ± 3 nm. In both sample B and sample C, the size distribution extends from 10 nm to 28 nm, but sample C has a relatively higher concentration of larger particles than sample B.

As with TEM imaging, particles with the organic surfactant present problems for obtaining high quality AFM images; indeed even with the dilution process, excess surfactant tends to remain on the surface of the silicon wafer (Fig. 2), making it difficult to judge precisely the height above the surface. The surfactant also collects around the particles blurring the edges. However, the images were of sufficient contrast to run the size analysis. Sample A showed multiple 15 nm particles with some variation from 15 nm of the order of 4 nm. Several large aggregates were also visible,

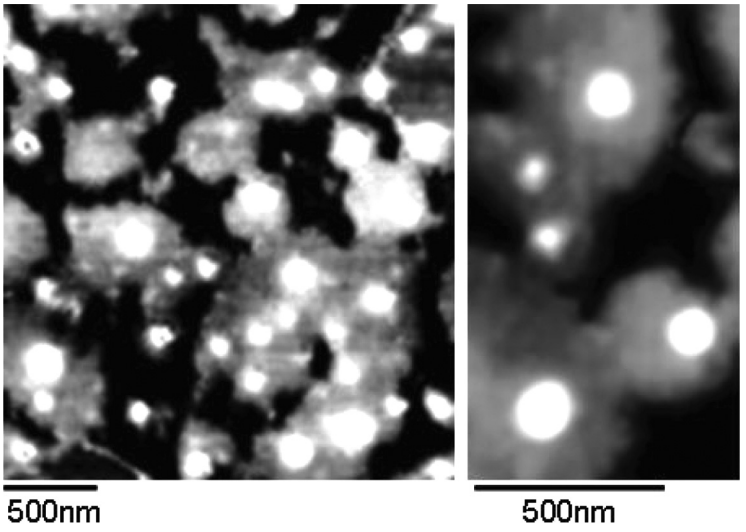

Figure 2. AFM images of ferroelectric Barium Titanate nanoparticles from sample A. The nanoparticles are clearly visible in the images as is the organic matter.

but it is not clear if these originated in the solution or were the results of evaporating the solvent on the AFM substrate. Particles from sample B were estimated as being 12 ± 4 nm and from sample C as 20 nm and 10 nm diameter (± 4 nm) on average.

All samples were then investigated in the Nanosight^{TM} imaging system. The resolution of Nanosight^{TM} is dependent upon the viscosity of the solvent used and the refractive index of the material under investigation. All the samples were tested, but the system was only able to determine the size distribution in sample C. This had a peak at approximately 30 nm that extended out to 50 nm, but larger aggregates were also recorded. As can be seen from Table 1, there is excellent agreement between the results from TEM and SSAFM imaging techniques. The exact peak of the size distributions are within 2 nm of each other, despite the smaller number of particles available to analyse with SSAFM. However, there appears to be a discrepancy between these two methods and the Nanosight^{TM} data. Although we used a low viscosity solvent, the best resolution achieved was approximately 25 nm which would explain the lack of reliable results using nanosight for the samples with smaller nanoparticles (samples A and B). Sample C, with the largest particles according to the other two methods, had the particles size determined as 30 nm. Furthermore, Nanosight^{TM} measures the hydrodynamic size of the particles, instead of the physical size. The organic surfactant attached to the particles could lead to increased effective particle size and lead to the measured value of 30 nm for sample C and the single peak observed. However, it is worth noting that the Nanosight data confirm sample C as having the largest nanoparticles.

3.2. *Electro-Optics Results and Discussion*

Following the size and shape analysis, the investigation of dielectric anisotropy and refractive index anisotropy measurements was carried out to determine how physical parameters affect electro-optic performance of suspensions. As can be seen in Figure 3 and Table 2, all of the $BaTiO_3$ nanoparticles suspensions have increased dielectric anisotropy, as compared to pure TL205 and MLC6815. The dielectric anisotropy increases with voltage and levels off at approximately 30 V. At 0 V the perpendicular component of the dielectric permittivity is measured, which is the smaller of the two dielectric components. As the voltage is increasing, the liquid crystal reorients and the larger, parallel component of the dielectric permittivity is accessed. As can be seen from Figure 3, with increasing voltage, the dielectric anisotropy increases from zero to a steady-state value. Table 2 shows that the largest increase for each liquid crystal was from the sample C. The dielectric anisotropy of TL205 increased by

Table 1. Average sizes of $BaTiO_3$ nanoparticles determined by three imaging techniques (AFM, TEM and Nanosight^{TM})

Imaging method	Sample A $BaTiO_3$ nanoparticles	Sample B of $BaTiO_3$ nanoparticles	Sample C of $BaTiO_3$ nanoparticles
TEM	15 ± 3 nm	12 ± 3 nm	12 nm and at 18 nm $\pm$ 3 nm
SSAFM	15 ± 4 nm	12 ± 4 nm	10 nm and 20 nm $\pm$ 4 nm
Nanosight^{TM}	N/A	N/A	30 nm

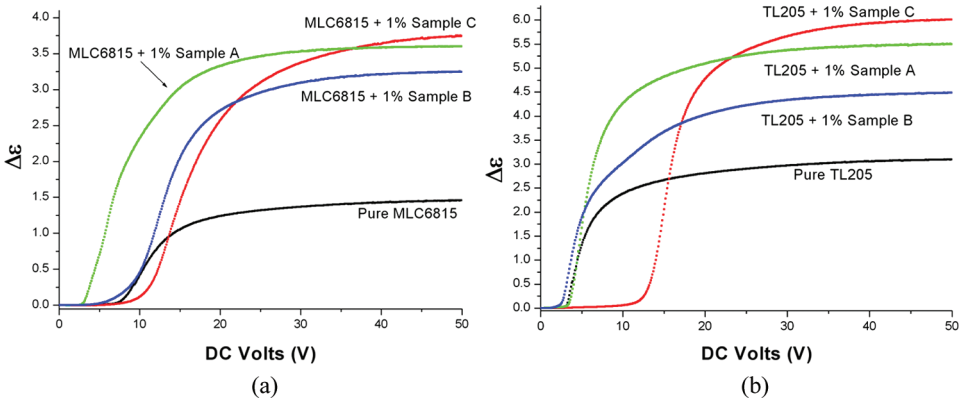

Figure 3. Measurements of dielectric anisotropy vs voltage. (3a) Pure MLC6815 and MLC6815 doped with 1% of each of the samples. (3b) Pure TL205 and Tl205 doped with 1% of each of the samples.

approximately 94% and MLC6815 by 156%. Sample A led to an increase in the dielectric anisotropy by 78% and 147%, in TL205 and MLC6815, respectively. The smallest increases were observed with sample B which were approximately 45% for TL205 and 122% for MLC6815. Overall, the magnitude of dielectric anisotropy enhancement is consistent with the nanoparticles size, with for example, the smallest nanoparticles (sample B) leading to the weakest enhancement.

It is also apparent in Figure 3 that the DC voltage threshold for reorientation is affected by the presence of nanoparticles. For example, for sample A in MLC6815, there is a definite shift to lower voltages. However, with sample C there is a shift to an increased threshold voltage. The shift to lower voltages can be attributed to an increased reorientation torque from the ferroelectric nanoparticles; indeed the lower AC field threshold in suspensions reported earlier confirms that [8]. However, as the dielectric permittivity measurements were carried out with an applied DC field, ions present in the suspensions will be driven to the substrates and can screen out the applied field. Doping with sample C appears to increase the concentration of ions and results in a higher DC field threshold.

The same liquid crystal response occurs in the refractive index measurements. Table 2 shows that all the suspensions have a larger refractive index anisotropy than the undoped TL205 and MLC6815 cells, respectively. There is clear trend for the

Table 2. Dielectric and optical anisotropy of TL205 and MLC6815 doped with 1% of each of the samples

TL205			MLC6815		
	$\Delta\varepsilon$	Δn		$\Delta\varepsilon$	Δn
Undoped TL205	3.09	0.21	Undoped MLC6815	1.46	0.05
Sample A + TL205	5.5	0.25	Sample A + MLC6815	3.6	0.07
Sample B + TL205	4.48	0.23	Sample B + MLC6815	3.24	0.06
Sample C + TL205	6.01	0.26	Sample C + MLC6815	3.74	0.08

largest particles (sample C) to lead to the strongest enhancement of refractive index anisotropy. With sample C, the optical anisotropy of TL205 increased by approximately 23% and MLC6815 by 60%. Sample A doping led to an increase of 19% and 40%; the smallest increases were from sample B which, namely were 10% and 20% for TL205 and MLC6815, respectively.

4. General Discussion

While both TEM and SSAFM techniques were able to identify the shape and size of nanoparticles, TEM offers the advantage of analysing hundreds of particles at once with a resolution of 3 nm, so size distributions can also be estimated. AFM images agree with the TEM results and provide confirmation of the data from TEM, however, far fewer particles can be analysed at the same time. Any size distribution determined from AFM alone would not be as robust. Nanosight^{TM} can analyse hundreds of particles, however, the samples described here are at the limit of the system's resolution. Furthermore Nanosight^{TM} determines the hydrodynamic diameter of the particles; in the ferroelectric suspensions this is less relevant than the actual physical size of the particles.

The same trends relating nanoparticles size versus the electro-optic performance of the suspensions are apparent in two different liquid crystals, TL205 a high birefringence liquid crystal and MLC6815, a low birefringence liquid crystal. In both liquid crystals, there is a significant increase in both dielectric and refractive index anisotropies, as the size of the doping particles increases. It can be suggested that larger nanoparticles have stronger dipoles, creating a considerable electric field around them [14] and significantly affecting the orientation of liquid crystals. However, they are sufficiently small, to remain as a single ferroelectric domain.

Adding ferroelectric nanoparticles to nematic liquid crystals causes substantial change of basic, nematic properties, which are directly related to the order parameter of the liquid crystal molecules. Indeed, dielectric anisotropy of liquid crystals $\Delta\varepsilon$ and birefringence Δn are proportional to the order parameter S [19], while liquid crystals; elastic constants, usually are proportional to S^2 [20]. Furthermore, small increase of temperature of transition to the isotropic phase, T_c, reported earlier [14] can increase order parameter according to the Maier-Saupe theory for the suspensions [19]. However, the limitation of this approach is that it does not consider the orientational distribution of the nanoparticles themselves. Such theory on the statistical mechanics of ferroelectric nanoparticles in liquid crystals was proposed recently [21]. It is based specifically on the orientational distribution of the nanoparticle dipole moments. This distribution is characterised by a separate orientational order parameter, which interacts with the orientational order of the liquid crystals and stabilises the nematic phase. The coupling strength between the two order parameters was estimated and also predicted an increase in T_c, in good agreement with experiments. Such enhancement occurs even when electrostatic interactions are partially screened by moderate concentrations of ions in the liquid crystals. More detailed theory and the importance of ions have to be considered further. Indeed, as shown in Figure 3, ions can play a substantial role in reorientation condition. For example, the higher DC voltage threshold seen for sample C could be the result of increased ion concentration screening out the effect of the applied field.

Finally, it is also worth noting that the suspensions and the electro-optic measurements have long term stability. For example, the measurements in TL205

suspensions were repeated nine months after the initial experiments and excellent agreement with the initial data was observed.

5. Conclusions

Size of ferroelectric nanoparticles produced by milling techniques and covered by oleic acid is best determined by using different imaging methods. TEM proved to be the most reliable in determining the average size and the distribution of particles and it also allows for a large numbers of particles to be imaged at high resolution and analysed. Three samples with different sizes of $BaTiO_3$ particles were mixed with liquid crystals TL205 and MLC6815 to create suspensions containing 1% (by weight) nanoparticles. It was demonstrated that both dielectric and optical anisotropy increase with increasing particle size.

Acknowledgments

The authors are very grateful to Anatoly Gluyshchenko and Dean Evans for providing us with planetary ball milled nanoparticles; Victor Reshetnyak, Yuri Reznikov and Geoffrey Luckhurst for useful discussions and advice regarding the data analysis. Financial support for this was provided by COI MOD.

References

[1] Diorio, N. J., Fisch, M. R., & West, J. W. (2002). *Liquid Crystals*, *29*, 589.
[2] Kossyrev, P. A. *et al*. (2005). *Nano Letters*, *5*, 1978.
[3] Muller, J. *et al*. (2002). *App. Phys. Lett.*, *81*, 171.
[4] Cook, G. *et al*. (2003). *Proc. SPIE* 5213, 63.
[5] Pagliusi, P., & Cipparrone, G. (2002). *Journal of Applied Physics*, *92*, 4863.
[6] Pagliusi, P., & Cipparrone, G. (2002). *App. Phys. Lett.*, *80*, 168.
[7] Dyadyusha, A., Kaczmarek, M., & Gilchrist, G. (2006). *Mol. Cryst. Liq. Cryst.*, *446*, 261.
[8] Reznikov, Y. *et al*. (2003). *App. Phys. Lett.*, *82*, 1917.
[9] Buchnev, O. *et al*. (2007). *J. Opt. Soc. Am. B*, *24*, 1512.
[10] Cook, G. *et al*. (2008). *Optics Express*, *16*, 4015.
[11] Kaczmarek, M., Buchnev, O., & Nandhakumar, I. (2008). *App. Phys. Lett.*, *92*, 103307.
[12] Kreuzer, M. *et al*. (1993). *App. Phys. Lett.*, *62*, 1712.
[13] Ouskova, E. *et al*. (2003). *Liquid Crystals*, *30*.
[14] Li, F. *et al*. (2006). *Phys. Rev. Lett.*, *97*, 147801.
[15] Zhong, W. L. *et al*. (1994). *Phys. Rev. B*, *50*, 12375.
[16] Kobayashi, Y. *et al*. (2004). *Journal of Sol-Gel Science and Technology*, *29*, 49.
[17] Atkuri, H. *et al*. (2009). *Journal of Optics A: Pure and Applied Optics*, *11*, 024006.
[18] Haase, W., & Poetzsch, D. (1976). *Molec. Cryst. Liq. Cryst.*, *38*, 77.
[19] Blinov, L. (1983). *Electro-optical and magneto-optical properties of liquid crystals*, Wiley.
[20] Stephen, M. J., & Straley, J. P. (1974). *Rev. Mod. Phys*, *46*, 617.
[21] Lopatina, L. M., & Selinger, J. V. (2009). *Phys. Rev. Lett.*, *102*, 197802.